ISSN 1674-1056
http://cpb.iphy.ac.cn
http://iopscience.iop.org/cpb
中国物理 B
Chinese Physics
中国物理
Chinese Physics B

Plasmon mediated entanglement dynamics of distant quantum dots

Misbah Qurban, Rabia Tahira, Guo-Qin Ge(葛国勤), Manzoor Ikram

Citation: Chin. Phys. B . 2019, 28(3): 030304. **doi:** 10.1088/1674-1056/28/3/030304
Journal homepage: http://cpb.iphy.ac.cn; http://iopscience.iop.org/cpb

What follows is a list of articles you may be interested in

The entanglement of deterministic aperiodic quantum walks

Ting-Ting Liu(刘婷婷), Ya-Yun Hu(胡亚运), Jing Zhao(赵静), Ming Zhong(钟鸣), Pei-Qing Tong(童培庆)

Chin. Phys. B . 2018, 27(12): 120305. **doi:** 10.1088/1674-1056/27/12/120305

Ultra-thin and light-weight spoof surface plasmon polariton coupler achieved by broadside coupled split ring resonators

Ya Fan(范亚), Jia-Fu Wang(王甲富), Hua Ma(马华), Yong-Feng Li(李勇峰), Ming-De Feng(冯明德), Shao-Bo Qu(屈绍波)

Chin. Phys. B . 2018, 27(10): 100304. **doi:** 10.1088/1674-1056/27/10/100304

Entangled-photons generation with quantum dots

Yuan Li(李远), Fei Ding(丁飞), Oliver G Schmidt

Chin. Phys. B . 2018, 27(2): 020307. **doi:** 10.1088/1674-1056/27/2/020307

Performance of superconducting nanowire single-photon detector with the fan coupling antenna array

Wang Yu-Jue, Ding Tian, Ma Hai-Qiang, Jiao Rong-Zhen

Chin. Phys. B . 2014, 23(6): 060308. **doi:** 10.1088/1674-1056/23/6/060308

Mesoscopic entangled coherent states implemented with a circuit quantum electrodynamics system

Zhao Ying-Yan, Jiang Nian-Quan

Chin. Phys. B . 2013, 22(5): 050308. **doi:** 10.1088/1674-1056/22/5/050308

Plasmon mediated entanglement dynamics of distant quantum dots*

Misbah Qurban[1,2,3,4], Rabia Tahira[1], Guo-Qin Ge(葛国勤)[1,†], and Manzoor Ikram[1,2]

[1] School of Physics, Huazhong University of Science and Technology, Wuhan 430074, China
[2] National Institute of Lasers and Optronics, Nilore, Islamabad 45650, Pakistan
[3] Department of Physics and Applied Mathematics, Pakistan Institute of Engineering and Applied Sciences, Nilore, Islamabad 45650, Pakistan
[4] Department of Physics, Fatima Jinnah Women University, The Mall, Rawalpindi, Pakistan

(Received 7 August 2018; revised manuscript received 8 January 2019; published online 26 February 2019)

We investigate the time evolution of entanglement between two quantum dots in an engineered vacuum environment such that a metallic nanoring having a surface plasmon is placed near the quantum dots. Such engineering in environment results in oscillations in entanglement dynamics of the quantum dots systems. With proper adjustment of the separation between the quantum dots, entanglement decay can be stabilized and preserved for longer time than its decay without the surface plasmons interactions.

Keywords: entanglement production and manipulation, entanglement dynamics, surface plasmon, quantum dots

PACS: 03.67.Bg, 03.65.Ud, 73.20.Mf **DOI:** 10.1088/1674-1056/28/3/030304

1. Introduction

Entanglement, a characteristic trait of the quantum theory, plays a vital role in fundamental tests of quantum mechanics as well as in the practical utilization through the emerging field of quantum informatics.[1] However, quantum information processing is facing many stringent challenges. These include the efficient high fidelity generation of many types of entangled states through diverse technologies like spin systems, flying photon qubits,[2] superconducting qubits, and atom field cavity quantum electro-dynamics (QED) systems.[3] Further, the fatal problem is the fragile nature of the engineered entangled states as they are prone to the decoherence threat. Thus the quantum information processing time is effectively constrained by the corresponding decoherence time, a threat effectively terminates the quantum process through quantum to classical transition. Under this scenario, the dynamical decay explorations, protection, and studies related to the stabilization strategies for the entanglement become vitally important.[4,5]

Speaking specifically in the context of solid state systems, one is referred to the recent demonstrations of entanglement generation between the spin of the single quantum dot and a single emitted photon, microcavity enhanced single-photon emission from single semiconductor quantum dots,[6] entangled photon generation with quantum dots,[7] teleportation of a photon over a spin qubit, as well as engineering of a heralded entanglement for spatially separated hole spins.[8] These promising results can be considered as a milestone towards the envisioned solid state based quantum networks provided that the resources being utilized here, i.e., entanglement, can be stabilized and protected against decays and the decoherence. Many working strategies are being tested and implemented in this regard. For example, it has been demonstrated that under a certain specific scenario, the system environment interaction that generally leads to decoherence can equally be controlled in a manner yielding stable entangled states.[9–11] Many theoretical proposals are raised for utilizing this phenomenon of dissipative-induced entanglement to cater the situation where quantum-dots interact with the plasmonic system.[12–17] In this regard, a broad distribution of surface plasmonic metallic wire guiding them along its axis in analogy with the optical modes of a dielectric fiber has been proposed.[18,19]

However, operational analogy being quite correct does offer certain fundamental differences as compared to dielectric waveguides.[20] Here the thin wire can efficiently sustain the surface plasmon propagation modes localized transversely within the dimension matching the wire radius r. This is interestingly true even for the cases with r much smaller than the optical wavelengths.[21] Such sub-wavelength localization consequently yields drastic enhancement in the optical field intensity, a parameter contributing to the high enough coupling of the quantum dots with the fields.[22,23] Moreover, the motion of surface plasmon modes usually stays at the moderate level as a consequence of the highly reduced velocities contributed by the charge density waves.[24–26] Such an effective interaction initiated by dissipative plasmon resonances in metal nano-particles, wires, or waveguides has already been shown in between the pair of two-level quantum dots placed in the vicinity of the system[27] in a manner much similar to the case of atoms entangled via a cavity field.[28] Here, in this case, the entanglement emerges spontaneously as a con-

*Project supported by the National Natural Science Foundation of China (Grant Nos. 11274132 and 11550110180).
†Corresponding author. E-mail: gqge@hust.edu.cn
© 2019 Chinese Physical Society and IOP Publishing Ltd

sequence of the common coupling of the plasmonic nanostructures, unavoided by any post-selective measurements or any specific engineering of the relevant environment.[29] Such fruitful entangled correlation among quantum dots can, however, be materialized through diverse techniques based on altogether different methodologies.[30–33] This evident interest of the working community in the plasmonics based QDs entanglements is thoroughly justified on utilitarian grounds as such systems are technically much easier to handle and manipulate compared to their counterparts that generally need either atom/ion traps or cryogenic temperature. Moreover, such plasmonic based QDs can be easily and efficiently integrated with rest of the nanophotonics gadgets, hinting the near future feasibility for the complex multi qubit communicational or computational quantum networks on just a miniature sized chip.

Therefore recent developments in the plasmonics and quantum information science motivate to study the entanglement dynamics in a system consisting of two QDs coupled to a metal nanoring surface plasmon (SP). The idea of our work is inspired by a recent proposal showing single surface plasmon in a metallic nanoring coupled to two quantum dots,[34] where they considered both the QDs initially in ground state and a SP in clockwise mode and showed the maximum of the entanglement occurring at the appropriate values of the inter-dot distances and coupling strengths. Here we apply the same model in order to stabilize the entanglement dynamics among the quantum dots by considering a metallic nanoring near the maximally entangled QDs interacting with the surface plasmon modes of the nanoring.

The paper is organized as follows. In Section 2, we present our model of two entangled QDs placed near a metallic nanoring. In Section 3, we discuss different cases of maximally entangled states and their dynamics when these QDs interact with the two modes of the surface plasmons with and without decoherence of QDs and SPs to the vacuum environment. Summary and conclusion are presented in Section 4.

2. Model

We consider two semiconductor QDs, initially prepared in entangled states, positioned near a metal nanoring having a surface plasmon in clockwise mode k as shown in Fig. 1. Consider R as a circular cross-section of the nanoring, then in the nanowire limit, $|k|R \ll 1$, only the fundamental mode of SP exists.[35] Thus the quantum-dot–nanoring system can be simplified as the two-level atoms in a resonator having $+k$ and $-k$ modes of radiation, as the right and left propagating wave vectors along the resonator axis, respectively. In case of the quantum-dot–nanoring system, the $+k$ mode of the SP is considered as the incident SP from a evanescently coupled waveguide photon propagation clockwise and the $-k$ mode as the counterclockwise mode of the SP resulting from the reflection of the $+k$ SP mode from QD. The Hamiltonian of the system can be written as[34]

$$\begin{aligned} H &= \hbar \sum_{j=1,2} \omega_{0j} \sigma_j^+ \sigma_j^- + \hbar \sum_{k'=k,-k} \omega_{k'} a_{k'}^\dagger a_{k'} \\ &\quad + \hbar [\mu_1 \sigma_1^+ a_k + \mu_2 \sigma_2^+ a_k \mathrm{e}^{\mathrm{i}kd} \\ &\quad + \mu_1 \sigma_1^+ a_{-k} + \mu_2 \sigma_2^+ a_{-k} \mathrm{e}^{\mathrm{i}k(S-d)} + \mathrm{H.C.}], \end{aligned} \tag{1}$$

where the first two terms are the free part Hamiltonian of the QDs and SP, respectively. $\hbar\omega_{0j}$ is the energy of the j^{th} QD, σ_j^+ (σ_j^-) is the raising (lowering) operator of the j^{th} QD with ground and excited states represented as $|g_j\rangle$ and $|e_j\rangle$, respectively, while $\omega_{k'}$ is the frequency of the k'-mode of SP, and a_k ($a_k^\dagger$) is the annihilation (creation) operator of the plasmon field. The remaining terms in Hamiltonian (1) represent the interaction of two QDs with clockwise $(+k)$ and anticlockwise $(-k)$ modes of the SP, where μ_1, μ_2 are the coupling strengths between the SP and QDs, d is the separation between the two QDs, and S is the circumference of the metal nanoring. In the nanowire limit, we assume the existence of only the fundamental mode of SP and hence $kS = 2\pi$. Therefore the above Hamiltonian reduces to

$$\begin{aligned} H &= \sum_{J=1,2} \omega_{0j} \sigma_j^+ \sigma_j^- + \hbar \sum_{k'=k,-k} \omega_{k'} a_{k'}^\dagger a_{k'} \\ &\quad + \hbar \sum_{k'=k,-k} \left(\mu_1 \sigma_1^+ a_{k'} + \mu_2 \sigma_2^+ a_{k'} \mathrm{e}^{\mathrm{i}k'd} + \mathrm{H.C.} \right). \end{aligned} \tag{2}$$

It is convenient to work in the interaction picture Hamiltonian given as

$$\begin{aligned} H_{\mathrm{I}} &= \hbar \sum_{k'=k,-k} \left(\mu_1 \sigma_1^+ a_{k'} \mathrm{e}^{\mathrm{i}(\omega_{01}-\omega_{k'})t} \right. \\ &\quad \left. + \mu_2 \sigma_2^+ a_{k'} \mathrm{e}^{\mathrm{i}(\omega_{02}-\omega_{k'})t + \mathrm{i}k'd} + \mathrm{H.C.} \right). \end{aligned} \tag{3}$$

This interaction Hamiltonian describes the QD–SP interaction in the dipole and rotating wave approximation (RWA), i.e., if the system is in close resonance then $\omega_{0j} \simeq \omega_{k'}$ and the frequencies $\omega_{0j} + \omega_{k'}$ are much larger than the other frequencies $\omega_{0j} - \omega_{k'}$, therefore the terms with $\mathrm{e}^{\pm\mathrm{i}(\omega_{0j}+\omega_{k'})}$ are neglected. We consider the QDs transitions in resonance with the frequencies of the SP modes, i.e., $\omega_{01} = \omega_{02} \approx \omega_k = \omega_{-k}$. Thus under resonance condition, the interaction picture Hamiltonian reduces to

$$H_{\mathrm{I}} = \hbar \sum_{k'=k,-k} \left(\mu_1 \sigma_1^+ a_{k'} + \mu_2 \sigma_2^+ a_{k'} \mathrm{e}^{\mathrm{i}k'd} + \mathrm{H.C.} \right). \tag{4}$$

The Hamiltonian in Eq. (4) does not include the effect of decoherence due to weak interaction of the system of QDs and SP with the environment compared to the interaction among QDs and SP modes. However if we include the system–environment interaction resulting in the decay of QDs and SP modes in vacuum, then under the condition that no photon is detected either by the spontaneous emission of QDs or decay

of any of the SP mode in vacuum, the evolution of the system of QD–SP is governed by the conditional Hamiltonian[36–40]

$$H_{\rm con} = H_{\rm I} - {\rm i}\frac{\hbar}{2}\sum_{j=1}^{2}\gamma_j \left|e_j\right\rangle\left\langle e_j\right| - {\rm i}\frac{\hbar}{2}\sum_{k'=k,-k}\Gamma_{k'}a_{k'}^{\dagger}a_{k'}, \quad (5)$$

where γ_j and $\Gamma_{k'}$ are the decay rates of the $j^{\rm th}$ QD and the $k^{\rm th}$ mode of SP, respectively, defined under the Markov approximation.[41]

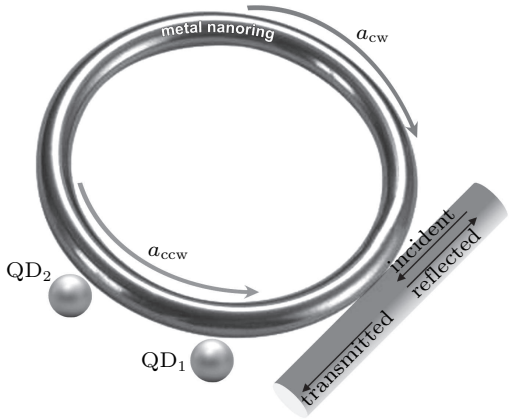


Fig. 1. Schematics diagram of two quantum dots coupled to a metal nanoring surface plasmon.

To study the entanglement dynamics of the system of two QDs, a quantitative measure of entanglement is necessary. For any bipartite entangled system, Wootters concurrence is a convenient method, defined as $E(t) = {\rm Max}\left\{0, \sqrt{\lambda_1} - \sqrt{\lambda_2} - \sqrt{\lambda_3} - \sqrt{\lambda_4}\right\}$, where λ_i are the eigenvalues of matrix $\rho_{\rm s}\widetilde{\rho}_{\rm s}$ with $\widetilde{\rho}_{\rm s} = (\sigma_y \otimes \sigma_y)\rho_{\rm s}^{*}(\sigma_y \otimes \sigma_y)$ arranged in descending order.[42] To obtain the density matrix ($\rho_{\rm s}$) of the QDs system, we first solve the equations of probability amplitudes of the state vector of QDs and SPs subject to initial conditions of QDs and SP and then take the trace over two modes of SPs. Here we consider different two-qubit initial states of the two QDs, and investigate the entanglement dynamics of the QDs system due to SP assisted continual mediation.

3. Entanglement dynamics

Here we analyze entanglement dynamics of initially entangled states of two QDs coupled to the SP of a metallic nanoring with the whole system being surrounded by a vacuum environment. We consider all four EPR states among QDs here.

Case 1 Let us assume one QD in the excited state while the other in the ground state with equal probability forming a maximally entangled state among the two QDs as $\left(\left|e_1, g_2\right\rangle \pm \left|g_1, e_2\right\rangle\right)/\sqrt{2}$. These QDs are placed near a metallic nanoring having a SP in clockwise $+k$ mode. Thus the QD–SP system can initially be written as

$$\left|\psi^{\pm}(0)\right\rangle = \frac{1}{\sqrt{2}}\left(\left|e_1, g_2\right\rangle \pm \left|g_1, e_2\right\rangle\right) \otimes \left|1_k, 0_{-k}\right\rangle. \quad (6)$$

The state of the system after the interaction of SP with QDs due to various processes such as transmission, reflection, absorption, and amplification of SP in QDs can be written as

$$\begin{aligned}\left|\psi(t)\right\rangle \;=\; & C_1(t)\left|e_1, e_2, 0_k, 0_{-k}\right\rangle + C_2(t)\left|e_1, g_2, 1_k, 0_{-k}\right\rangle \\ & + C_3(t)\left|e_1, g_2, 0_k, 1_{-k}\right\rangle + C_4(t)\left|g_1, e_2, 1_k, 0_{-k}\right\rangle \\ & + C_5(t)\left|g_1, e_2, 0_k, 1_{-k}\right\rangle + C_6(t)\left|g_1, g_2, 2_k, 0_{-k}\right\rangle \\ & + C_7(t)\left|g_1, g_2, 1_k, 1_{-k}\right\rangle + C_8(t)\left|g_1, g_2, 0_k, 2_{-k}\right\rangle, \quad (7)\end{aligned}$$

where $C_i(t)$ are the probability amplitudes of the basis defined in the state vector $\left|\psi(t)\right\rangle$ above. Let the system of QDs–SP be surrounded by the environment with system environment coupling assumed weak as compared to the coupling between the QDs and SP. For such a situation, we can find the derivatives of the probability amplitudes $C_i(t)$ from Schrödinger equation $\frac{\rm d}{{\rm d}t}\left|\psi(t)\right\rangle = -\frac{\rm i}{\hbar}H_{\rm con}\left|\psi(t)\right\rangle$ as given in Appendix A.

We solve the equations of the probability amplitudes numerically and take trace over all the plasmonic modes to obtain the following density matrix for the two QDs:

$$\rho_{\rm QD}^{(1)}(t) = \begin{pmatrix} |C_1|^2 & 0 & 0 & 0 \\ 0 & |C_2|^2 + |C_3|^2 & C_2C_4^{*} + C_3C_5^{*} & 0 \\ 0 & C_2^{*}C_4 + C_3^{*}C_5 & |C_4|^2 + |C_5|^2 & 0 \\ 0 & 0 & 0 & |C_6|^2 + |C_7|^2 + |C_8|^2 \end{pmatrix}, \quad (8)$$

where $C_i = C_i(t)$. For entanglement dynamics, we need the eigenvalues of the matrix $\rho_{\rm QD}^{(1)}(\sigma_y \otimes \sigma_y)\rho_{\rm QD}^{(1)*}(\sigma_y \otimes \sigma_y)$, which are oscillatory due to the interaction of QDs with SPs. Due to this oscillatory nature of the eigenvalues, the entanglement of the QDs system can be found using

$$E_1(t) = {\rm Max}\left\{0, \Lambda_1(t), \Lambda_2(t)\right\}, \quad (9)$$

where

$$\begin{aligned}\Lambda_1(t) \;=\; & 2\Big(\left|C_2(t)C_4^{*}(t) + C_3(t)C_5^{*}(t)\right| \\ & - \sqrt{|C_1(t)|^2\left(|C_6(t)|^2 + |C_7(t)|^2 + |C_8(t)|^2\right)}\Big), \quad (10)\end{aligned}$$

$$\Lambda_2(t) \;=\; 2\sqrt{\left(|C_2(t)|^2 + |C_3(t)|^2\right)\left(|C_4(t)|^2 + |C_5(t)|^2\right)}. \quad (11)$$

Entanglement dynamics of the QDs systems with and without decoherence are shown in Figs. 2 and 3 for the QDs–SP states $|\psi^+(t)\rangle$ and $|\psi^-(t)\rangle$, respectively. The concurrence plots are different for the two states. We see oscillations in entanglement in both cases due to the interaction of QDs with the two modes of the SP. Entanglement starts from its maximum value and during their oscillations it again achieves maxima periodically. For $|\psi^+(t)\rangle$, the frequency of oscillations decreases with the increase in the separation between the QDs with periodical increase to the maximum value of entanglement until one reaches the QDs separation $kd = \pi$, where it sustains its maximum value. For the singlet state $|\psi^-(t)\rangle$, the behavior of entanglement dynamics is reversed as that of $|\psi^+(t)\rangle$ regarding the interdot distance. Here we note that the frequency of oscillation is fast at QDs separation $kd = \pi$ and it decreases with decrease in the inter-dot separation and approaches a stable value when the QDs are very close to each other.

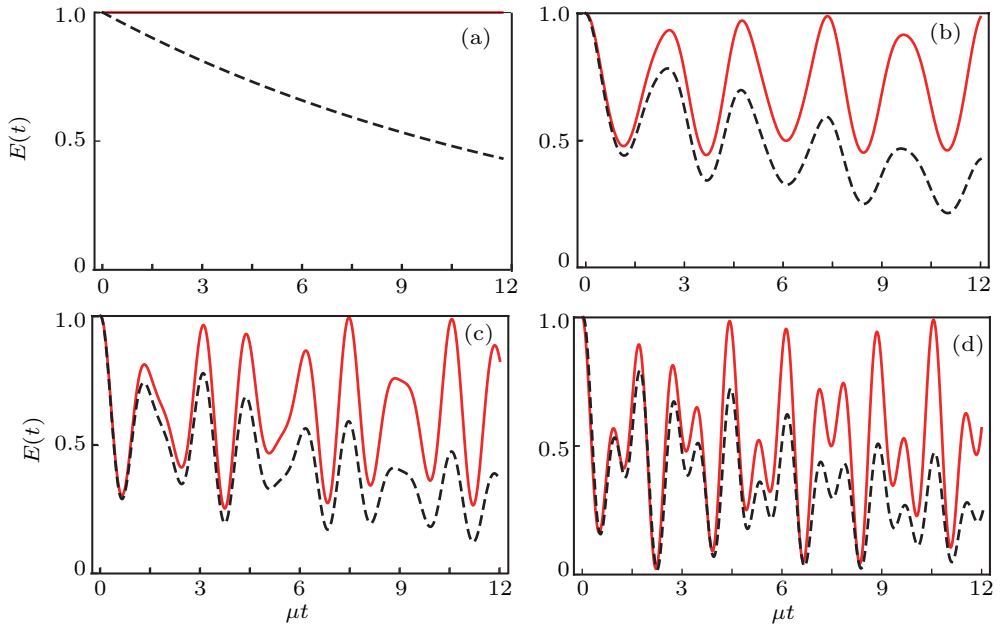


Fig. 2. Entanglement dynamics of two quantum dots with initial sate $|\psi^+(0)\rangle$ for interdot distances (a) $kd = \pi$, (b) $kd = 3\pi/4$, (c) $kd = \pi/2$, and (d) $kd = \pi/4$. Here we assume symmetric coupling $(\mu_1 = \mu_2 = \mu)$ and $\Gamma_k = \Gamma_{-k} = \gamma_1 = \gamma_2 = \gamma$. The solid red line represents $\gamma = 0$, and the dotted black line represents dynamics at $\gamma = \mu/30$.

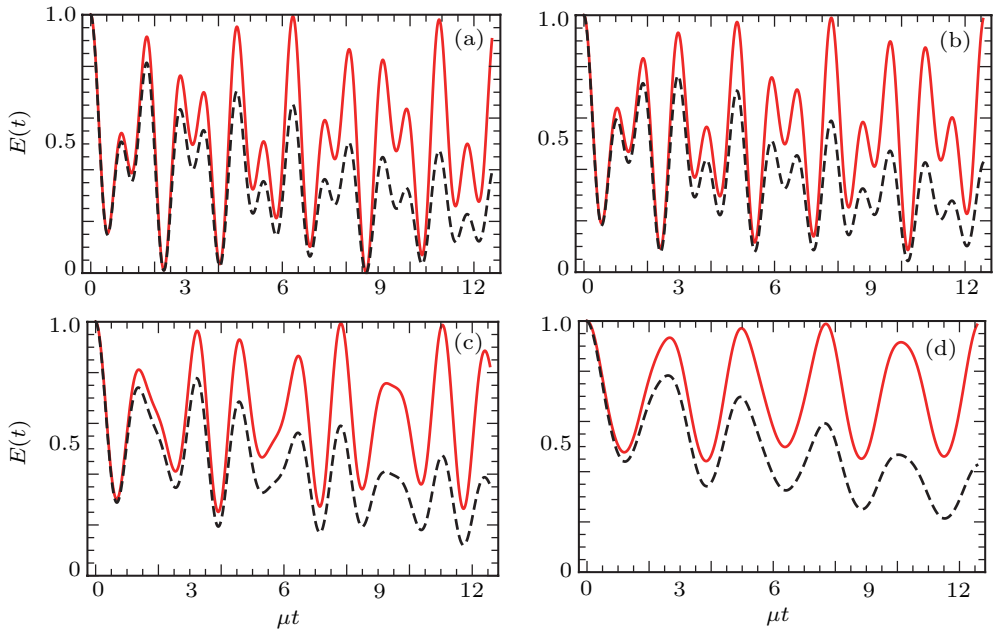


Fig. 3. Entanglement dynamics of two quantum dots with initial sate $|\psi^-(0)\rangle$ for interdot distance (a) $kd = \pi$, (b) $kd = 3\pi/4$, (c) $kd = \pi/2$, and (d) $kd = \pi/4$. Here we assume symmetric coupling $(\mu_1 = \mu_2 = \mu)$ and $\Gamma_k = \Gamma_{-k} = \gamma_1 = \gamma_2 = \gamma$. The solid red line represents $\gamma = 0$, and the dotted black line represents dynamics at $\gamma = \mu/30$.

Case 2 Let us assume that the QDs are initially in the maximally entangled state as $(|e_1,e_2\rangle+|g,g_2\rangle)/\sqrt{2}$ placed near a metallic nanoring having a SP in $+k$ mode. It therefore represents the combination of single and triple excitations cases. We have shown earlier that the single excitation, i.e., both the QDs in ground states and a SP in clockwise mode generate entanglement between QDs as well as among SP modes at some particular values of interdot distance kd and interactional parameter μt.[43] Here we consider the initial state of the QD–SP system

$$\left|\phi^{\pm}(0)\right\rangle=\frac{1}{\sqrt{2}}\left(|e_1,e_2\rangle\pm|g,g_2\rangle\right)\otimes|1_k,0_{-k}\rangle. \tag{12}$$

The basis due to transmission, reflection, absorption, amplification, and loss of plasmon in the environment can be expressed through the ansatz corresponding to arbitrary interaction time t as

$$\begin{aligned}
&|\phi(t)\rangle\\
=\;&D_1(t)|e_1,e_2,1_k,0_{-k}\rangle+D_2(t)|e_1,e_2,0_k,1_{-k}\rangle\\
&+D_3(t)|e_1,g_2,2_k,0_{-k}\rangle+D_4(t)|e_1,g_2,1_k,1_{-k}\rangle\\
&+D_5(t)|e_1,g_2,0_k,2_{-k}\rangle+D_6(t)|g_1,e_2,2_k,0_{-k}\rangle\\
&+D_7(t)|g_1,e_2,0_k,2_{-k}\rangle+D_8(t)|g_1,e_2,1_k,1_{-k}\rangle\\
&+D_9(t)|g_1,g_2,3_k,0_{-k}\rangle+D_{10}(t)|g_1,g_2,1_k,2_{-k}\rangle\\
&+D_{11}(t)|g_1,g_2,2_k,1_{-k}\rangle+D_{12}(t)|g_1,g_2,0_k,3_{-k}\rangle\\
&+D_{13}(t)|g_1,g_2,1_k,0_{-k}\rangle+D_{14}(t)|g_1,g_2,0_k,1_{-k}\rangle\\
&+D_{15}(t)|e_1,g_2,0_k,0_{-k}\rangle+D_{16}(t)|g_1,e_2,0_k,0_{-k}\rangle,
\end{aligned} \tag{13}$$

where $D_i(t)$ are the probability amplitudes corresponding to the basis mentioned above. The time derivatives of these probability amplitudes as obtained from the Schrödinger equation are shown in Appendix B. Following the same procedure as in case 1, the density matrix of the system of QDs alone can be obtained from the solutions of the probability amplitudes $D_i(t)$ and followed by taking the trace over all the SP modes as

$$\rho_{\mathrm{QD}}^{(2)}(t)=\begin{pmatrix}\rho_{11}(t)&0&0&\rho_{14}(t)\\0&\rho_{22}(t)&\rho_{23}(t)&0\\0&\rho_{32}(t)&\rho_{33}(t)&0\\\rho_{41}(t)&0&0&\rho_{44}(t)\end{pmatrix}, \tag{14}$$

where

$$\begin{aligned}
\rho_{11}(t)&=|D_1(t)|^2+|D_1(t)|^2,\\
\rho_{14}(t)&=D_1(t)D_{15}^*(t)+D_2(t)D_{16}^*(t),\\
\rho_{22}(t)&=|D_3(t)|^2+|D_4(t)|^2+|D_5(t)|^2+|D_{13}(t)|^2,\\
\rho_{23}(t)&=D_3(t)D_6^*(t)+D_4(t)D_7^*(t)+D_5(t)D_8^*(t)\\
&\quad+D_{13}(t)D_{14}^*(t),\\
\rho_{32}(t)&=\rho_{23}^*(t),\\
\rho_{33}(t)&=|D_6(t)|^2+|D_7(t)|^2+|D_8(t)|^2+|D_{12}(t)|^2,\\
\rho_{41}(t)&=\rho_{14}^*(t),\\
\rho_{44}(t)&=|D_9(t)|^2+|D_{10}(t)|^2+|D_{11}(t)|^2+|D_{12}(t)|^2\\
&\quad+|D_{15}(t)|^2+|D_{16}(t)|^2.
\end{aligned}$$

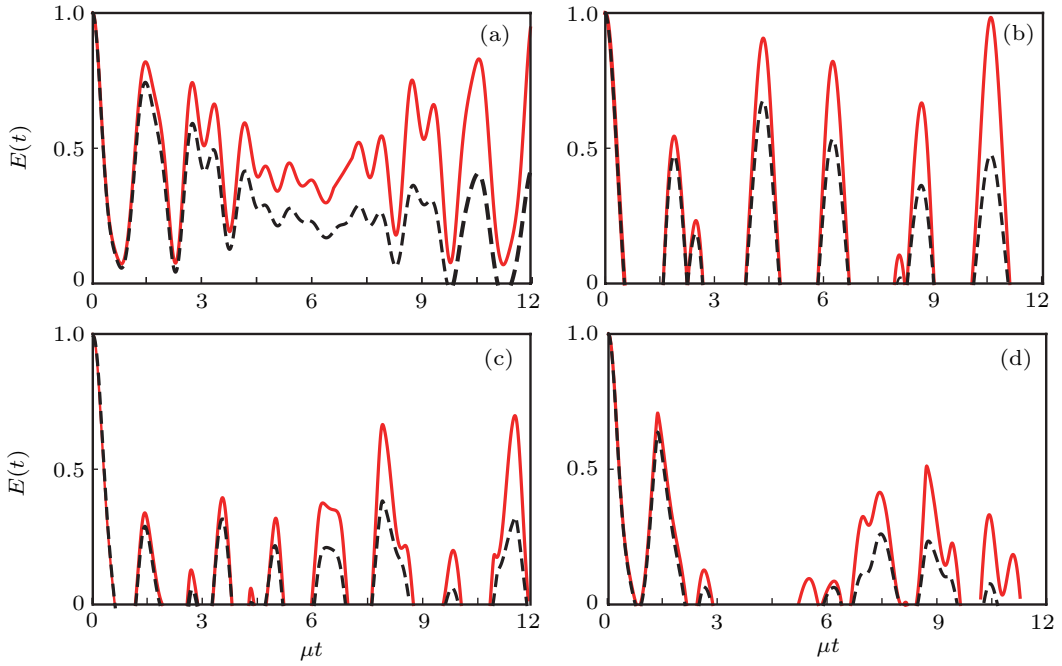


Fig. 4. Entanglement dynamics of two quantum dots with initial sate $|\phi^{\pm}(0)\rangle$ for interdot distance (a) $kd=\pi$, (b) $kd=\pi/2$, (c) $kd=\pi/8$ and (d) $kd=\pi/16$. Here we assume symmetric coupling $(\mu_1=\mu_2=\mu)$ and $\Gamma_k=\Gamma_{-k}=\gamma_1=\gamma_2=\gamma$. The solid red line represents $\gamma=0$, and the dotted black line represents dynamics $\gamma=\mu/30$.

The entanglement for this case is determined as

$$E_2(t) = \mathrm{Max}\{0, \Lambda_3(t), \Lambda_4(t)\}, \tag{15}$$

where

$$\Lambda_3(t) = 2\left(\sqrt{\rho_{11}(t)\rho_{44}(t)} - |\rho_{23}(t)|\right), \tag{16}$$

$$\Lambda_4(t) = 2\left(|\rho_{14}(t)| - \sqrt{\rho_{22}(t)\rho_{33}(t)}\right). \tag{17}$$

Figure 4 shows dynamics of the entangled state $|\phi^{\pm}(t)\rangle$ for interdot distances of $kd = \pi$, $\pi/2$, $\pi/8$, and $\pi/16$. We do not see any effect of phase factor here and both the states $|\phi^{+}(t)\rangle$ and $|\phi^{-}(t)\rangle$ behave exactly the same. Entanglement is again oscillatory because of QDs coupling with SP modes of the metallic nanoring. For interdot distance $kd = \pi$, entanglement does not vanish but it oscillates periodically contrary to the dynamics of the same state without SP. For interdot separation less than π, we see collapse and revivals of entanglement. Multiple peaks in the entanglement are due to the oscillatory behavior of the eigenvalues of the matrix $\rho_{\mathrm{QD}}^{(2)}(t)\,\widetilde{\rho}_{\mathrm{QD}}^{(2)}(t)$. One eigenvalue does not remain maximum for all time but when one eigenvalue decreases, the other increases and becomes maximum at some specific time during the evolution. Overall decay of entanglement is due to the coupling of the QDs and SP to the vacuum environment.

4. Discussion and conclusion

In summary, we have investigated entanglement dynamics between two quantum dots initially prepared in maximum entanglement and placed near a metallic nanoring, thus supporting the interactive scenario much akin to a cavity utilized for controlled atom–field interaction. All four maximally entangled Bell states among QDs are considered. We see the oscillatory behavior of entanglement dynamics in each case with oscillation frequency depending upon the interdot separation. The oscillatory behavior of entanglement between the QDs is due to the interaction of these QDs with the SP modes. Before the relaxation of the QDs, Rabi oscillations take place due to the coupling with the SP modes. These oscillations are similar to the two entangled atoms close together having dipole–dipole interaction. In each case we see stability in the entanglement dynamics at certain specific interdot separation contrary to the asymptotic dynamics of the entangled quantum dots coupled to the vacuum environment only. For the entangled state between QDs $(|e_1, e_2\rangle + |g_1, g_2\rangle)/\sqrt{2}$ with two QDs separated by $kd = \pi$, we see that damping of the entanglement does not vanish altogether but it periodically oscillates after reaching to its minimum at about 30% of maximum value. In case for other QDs separations kd less than π, we see collapse and revivals of entanglement not seen for the same state without the SP interaction of QDs.

Regarding experimental feasibility, we see that all the necessary ingredients in the present scheme including the metallic nanoring,[44,45] and precise placement of QDs with accuracy of 45 nm have already been experimentally realized.[46] For the realization of coupling between a metal nanoring SP and two/three QDs, colloidal CdSe/ZnS QDs and a silver nanoring are ideal since the excitation energy of CdSe/ZnS QDs is around 2–2.5 eV, compatible with the saturation plasma energy of the silver nanowire.[47] Considering only the fundamental mode of SP in nanoring cavity, the radius of silver nanoring should be around 100 nm. Dipole moment of QDs of the order of 0.5×10^{-28} C·m has been reported in literature.[48,49] Coupling constant μ of QDs and SP is proportional to the dipole moments of QDs and the field strength of the SP. Strong coupling of SP and QDs has been reported.[50] One of the major issues in this scheme is that SP inevitably experiences losses as it propagates along the nanowire which limits the generation of entanglement between QDs. In order to have strong coupling between QDs and SP, one needs to increase the Q-factor of the plasmonic modes. It not only increases the coupling between the SP and QDs but reduces the damping of plasmonic modes Γ_k and Γ_{-k}. Large dipole moments of the QDs, ultrahigh Purcell factor $(> 10^4)$ of the metallic nanoring,[51] and long propagation distance $(2.17\ \mathrm{mm})$[52] make our scheme experimentally realizable. Therefore the decay rates of QDs and SP can safely be taken as $\mu/30$ with the available technology. Further our results show that decay rates κ and $\Gamma_k = \Gamma_{-k}$ do not have any significant effects on the oscillatory behavior of the entanglement between QDs but it reduces the amount of entanglement only. Small decay rates due to high Q-factor and high Purcell factor support our proposal of entanglement preservation between QDs in the presence of SP modes. While measurement of the entanglement can be carried out using ultrafast optical tomography.[53] The present schematic can be straightforwardly intended to the multipartite case and, therefore, we quite optimistically believe that present work hints out towards a feasible strategy to engineer multipartite entangled networks and complex state morphologies.

Appendix A: Equations of motion of the probability amplitudes of $|\psi(t)\rangle$

The equations of motion of the probability amplitudes $C_i(t)$ of the state $|\psi(t)\rangle$ are

$$\begin{aligned}
\dot{C}_1(t) &= -\mathrm{i}[\mu_2(C_2(t)\,\mathrm{e}^{\mathrm{i}kd} + C_3(t)\,\mathrm{e}^{-\mathrm{i}kd}) \\
&\quad + \mu_1(C_4(t) + C_5(t))] - \frac{1}{2}\gamma_1 C_1(t), \\
\dot{C}_2(t) &= -\mathrm{i}[\mu_2^{*} C_1(t)\,\mathrm{e}^{-\mathrm{i}kd} + \mu_1(C_6(t) + \sqrt{2}C_7(t))] \\
&\quad - \frac{1}{2}(\gamma_1 + \Gamma_1)C_2(t),
\end{aligned}$$

$$\dot{C}_3(t) = -\mathrm{i}[\mu_2^* C_1(t)\mathrm{e}^{\mathrm{i}kd} + \mu_1(C_6(t)+\sqrt{2}C_8(t))] - \frac{1}{2}(\gamma_1+\Gamma_2)C_3(t),$$

$$\dot{C}_4(t) = -\mathrm{i}[\mu_1^* C_1(t) + \mu_2(C_6(t)\mathrm{e}^{-\mathrm{i}kd} + \sqrt{2}C_7(t)\mathrm{e}^{\mathrm{i}kd})] - \frac{1}{2}(\gamma_2+\Gamma_1)C_4(t),$$

$$\dot{C}_5(t) = -\mathrm{i}[\mu_1^* C_1(t) + \mu_2(C_6(t)\mathrm{e}^{\mathrm{i}kd} + \sqrt{2}C_8(t)\mathrm{e}^{-\mathrm{i}kd})] - \frac{1}{2}(\gamma_2+\Gamma_2)C_5(t),$$

$$\dot{C}_6(t) = -\mathrm{i}[\mu_1^*(C_2(t)+C_3(t)) + \mu_2^*(C_4(t)\mathrm{e}^{\mathrm{i}kd} + C_5(t)\mathrm{e}^{-\mathrm{i}kd})] - \Gamma_1 C_6(t),$$

$$\dot{C}_7(t) = -\mathrm{i}\sqrt{2}[\mu_1^* C_2(t) + \mu_2^* C_4(t)\mathrm{e}^{-\mathrm{i}kd}] - \frac{1}{2}(\gamma_1+\Gamma_2),$$

$$\dot{C}_8(t) = -\mathrm{i}\sqrt{2}[\mu_1^* C_3(t) + \mu_2^* C_5(t)\mathrm{e}^{\mathrm{i}kd}] - \Gamma_2 C_8(t).$$

Appendix B: Equations of motion of the probability amplitudes of $|\phi(t)\rangle$

The equations of motion of the probability amplitudes $D_i(t)$ of the state $|\phi(t)\rangle$ are

$$\dot{D}_1(t) = -\mathrm{i}[\mu_2(D_3(t)\mathrm{e}^{-\mathrm{i}kd} + \sqrt{2}D_4(t)\mathrm{e}^{\mathrm{i}kd}) + \mu_1 \times (D_6(t)+\sqrt{2}D_7(t))] - \frac{1}{2}(\gamma_1+\gamma_2+\Gamma_1)D_1(t),$$

$$\dot{D}_2(t) = -\mathrm{i}[\mu_2(D_3(t)\mathrm{e}^{\mathrm{i}kd} + \sqrt{2}D_5(t)\mathrm{e}^{-\mathrm{i}kd}) + \mu_1 \times (D_6(t)+\sqrt{2}D_8(t))] - \frac{1}{2}(\gamma_1+\gamma_2+2\Gamma_1)D_2(t),$$

$$\dot{D}_3(t) = -\mathrm{i}[\mu_2^*(D_1(t)\mathrm{e}^{\mathrm{i}kd} + D_2(t)\mathrm{e}^{-\mathrm{i}kd}) + \mu_1\sqrt{2} \times (D_9(t)+D_{10}(t))] - \frac{1}{2}(\gamma_1+2\Gamma_1)D_3(t),$$

$$\dot{D}_4(t) = -\mathrm{i}[\mu_2^*\sqrt{2}D_1(t)\mathrm{e}^{-\mathrm{i}kd} + \mu_1(D_{10}(t) + \sqrt{3}D_{11}(t))] - \frac{1}{2}(\gamma_1+\Gamma_1+\Gamma_2)D_4(t),$$

$$\dot{D}_5(t) = -\mathrm{i}[\mu_2^*\sqrt{2}D_2(t)\mathrm{e}^{\mathrm{i}kd} + \mu_1(D_4(t) + \sqrt{3}D_{12}(t))] - \frac{1}{2}(\gamma_1+2\Gamma_2)D_5(t),$$

$$\dot{D}_6(t) = -\mathrm{i}[\mu_1^*(D_2(t)+D_1(t)) + \sqrt{2}\mu_2(D_9(t)\mathrm{e}^{-\mathrm{i}kd} + D_{10}(t)\mathrm{e}^{\mathrm{i}kd})] - \frac{1}{2}(\gamma_2+2\Gamma_1)D_6(t),$$

$$\dot{D}_7(t) = -\mathrm{i}[\sqrt{2}\mu_1^* D_1(t) + \mu_2(D_{10}(t)\mathrm{e}^{-\mathrm{i}kd} + \sqrt{3}D_{11}(t)\mathrm{e}^{\mathrm{i}kd})] - \frac{1}{2}(\gamma_2+2\Gamma_2)D_7(t),$$

$$\dot{D}_8(t) = -\mathrm{i}[\sqrt{2}\mu_1^* D_2(t) + \mu_2(D_9(t)\mathrm{e}^{\mathrm{i}kd} + \sqrt{3}D_{12}(t)\mathrm{e}^{-\mathrm{i}kd})] - \frac{1}{2}(\gamma_2+\Gamma_1+\Gamma_2)D_8(t),$$

$$\dot{D}_9(t) = -\mathrm{i}[\mu_1^*(\sqrt{2}D_3(t)+D_5(t)) + \mu_2^*(\sqrt{2}D_6(t)\mathrm{e}^{\mathrm{i}kd} + D_8(t)\mathrm{e}^{-\mathrm{i}kd})] - \frac{3}{2}\Gamma_1 D_9(t),$$

$$\dot{D}_{10}(t) = -\mathrm{i}[\mu_1^*(\sqrt{2}D_3(t)+D_4(t)) + \mu_2^*(\sqrt{2}D_6(t)\mathrm{e}^{-\mathrm{i}kd} + D_7(t)\mathrm{e}^{\mathrm{i}kd})] - \frac{1}{2}(\Gamma_1+2\Gamma_2)D_{10}(t),$$

$$\dot{D}_{11}(t) = -\mathrm{i}\sqrt{3}[\mu_1^* D_4(t) + \mu_2^* D_7(t)\mathrm{e}^{-\mathrm{i}kd}] - \frac{1}{2}(2\Gamma_1+\Gamma_2)D_{11}(t),$$

$$\dot{D}_{12}(t) = -\mathrm{i}\sqrt{3}[\mu_1^* D_5(t) + \mu_2^* D_8(t)\mathrm{e}^{\mathrm{i}kd}] - \frac{3}{2}\Gamma_2 D_{12}(t),$$

$$\dot{D}_{13}(t) = -\mathrm{i}\mu_1[D_{15}(t)+D_{16}(t)] - \frac{1}{2}\Gamma_1 D_{13}(t),$$

$$\dot{D}_{14}(t) = -\mathrm{i}\mu_2[D_{15}(t)\mathrm{e}^{\mathrm{i}kd} + D_{16}(t)\mathrm{e}^{-\mathrm{i}kd}] - \frac{1}{2}\Gamma_2 D_{14}(t),$$

$$\dot{D}_{15}(t) = -\mathrm{i}[\mu_1^* D_{13}(t) + \mu_2^* D_{14}(t)] - \frac{1}{2}\gamma_1 D_{15}(t),$$

$$\dot{D}_{16}(t) = -\mathrm{i}[\mu_1^* D_{13}(t) + \mu_2^* D_{14}(t)\mathrm{e}^{\mathrm{i}kd}] - \frac{1}{2}\gamma_2 D_{16}(t).$$

References

[1] Nielsen M A and Chuang L I 2010 Quantum Computation and Quantum Information (New York: Cambridge University Press)
[2] Jefferson J H, Ramšak A and Rejec T 2008 *J. Phys.: Condens. Matter* **20** 164206
[3] Ikram M, Li F L and Zubairy M S 2007 *Phys. Rev. A* **75** 062336
[4] Xie M, Wu F, Fu P and Yang G 2015 *Quantum Information Processing* **14** 2077
[5] Schwartz M E K, Martin L, Flurin E, Aron C, Kulkarni M, Tureci E H and Siddiqi I 2016 *Phys. Rev. Lett.* **116** 240503
[6] Shou C and Lai X X 2014 *Physics* **43** 740
[7] Li Y, Ding F and Schmidt O G 2018 *Chin. Phys. B* **27** 020307
[8] Wagenknecht C, Li C M, Reingruber A, Bao X H, Goebei A, Chen Y A, Zhang Q, Chen K and Pan J W 2010 *Nat. Photon.* **4** 549
[9] Poyatos J F, Cirac J I and Zoller P 1996 *Phys. Rev. Lett.* **77** 4728
[10] Lin Y, Gaebler J P, Reiter F, Tan T R, Bowleer R, Sorensen A S, Leibfried D and Wineland D J 2013 *Nature* **504** 415
[11] Krauter H, Muschik C A, Jensen K, Wasilewski W, Petersen J M, Cirac J I and Polzik E S 2011 *Phys. Rev. Lett.* **107** 080503
[12] Tudela A G, Cano D M, Moreno E, Moreno L M, Tejedor C and Vidal F J G 2011 *Phys. Rev. Lett.* **106** 020501
[13] Cano D M, Tudela A G, Moreno L M, Vidal L M G, Tejedor C and Moreno E 2011 *Phys. Rev. B* **84** 235306
[14] He Y and Zhu K D 2012 *Nanoscale Res. Lett.* **7** 95
[15] He Y and Zhu K D 2013 *Quantum Info. Comput.* **13** 0324
[16] Ballestero C G, Vidal F J G and Moreno E 2013 *New J. Phys.* **15** 073015
[17] Lee C 2013 *New J. Phys.* **15** 083017
[18] Sanders A W 2006 *Nano Lett.* **6** 1822
[19] Ditlbacher H 2005 *Phys. Rev. Lett.* **95** 257403
[20] Nayak K P 2007 *Opt. Express* **15** 5431
[21] Haroche S and Raimond J M 2006 *Exploring the Quantum: Atoms, Cavities, Photons* (New York: Oxford University Press)
[22] Atwater H A 2007 *Sci. Am.* **296** 56
[23] Genet C and Ebbesen T W 2007 *Nature* **445** 39
[24] Chang D E, Sørensen A S, Hemmer P R and Lukin M D 2006 *Phys. Rev. Lett.* **97** 053002
[25] Takahara J, Yamagishi S, Taki H, Morimoto A and Kobayashi 1997 *Opt. Lett.* **22** 475
[26] Chang D E, S?rensen A S, Hemmer P R and Lukin M D 2007 *Phys. Rev. B* **76** 035420
[27] Artuso R D and Bryant G W 2013 *Phys. Rev. B* **87** 125423
[28] Nicolosi S, Napoli A, Messina A and Petruccione F 2004 *Phys. Rev. A* **70** 022511
[29] Tame M S, McEnery K R, Ozdemir S K, Lee J, Maier S A and Kim M S 2013 *Nat. Phys.* **9** 329
[30] Quiroga L and Johnson N F 1999 *Phys. Rev. Lett.* **83** 2270
[31] Bayer M, Hawrylak P, Hinzer K, Fafard S, Korkusinski M, Wasilewski Z R, Stern O and Forchel A 2001 *Science* **291** 451
[32] Wang X, Feng M and Sanders B C 2003 *Phys. Rev. A* **67** 022302
[33] Posazhennikova A, Birmuske R, Bruderer M and Belzig W 2012 *Phys. Rev. A* **88** 042302
[34] Chen G Y, Li C M and Chen Y N 2012 *Opt. Lett.* **37** 1337
[35] Lin Z R, Guo G P, Tu T, Li H O, Zou C L, Chen J X, Lu Y H, Ren X F and Guo G C 2010 *Phys. Rev. B* **82** 241401(R)

[36] Zheng S B 2005 *Phys. Rev. A* **71** 062335
[37] Zheng S B and Guo G C 2006 *Phys. Rev. A* **73** 032329
[38] Zheng S B and Guo G C 2006 *Phys. Rev. A* **73** 052328
[39] Zheng S B 2008 *Phys. Rev. A* **77** 044303
[40] Yang W L, Yin Z Q, Xu Z Y, Feng M and Oh C H 2011 *Phys. Rev. A* **84** 043849
[41] Scully M O and Zubairy M S 1997 *Quantum Optics* (Cambridge: Cambridge University Press)
[42] Wootters W K 1998 *Phys. Rev. Lett.* **80** 2245
[43] Qurban M, Ikram M, Ge G and Zubairy M S 2018 *J. Phys. B* **51** 155502
[44] Gomez D E, Vernon K C, Mulvaney P and Davis T J 2010 *Nano Lett.* **10** 274
[45] Liu S D, Yang Z, Liu R P and Li X Y 2011 *J. Phys. Chem. C* **115** 24469
[46] Ropp C, Probst R, Cummins Z, Kumar R, Berglund A J, Ragavan S R, Waks E and Shapiro B 2010 *Nano Lett.* **10** 2525
[47] Chen G, Lambert N, Chou C H, Chen Y N and Nori F 2011 *Phys. Rev. B* **84** 045310
[48] Mar J D, Baumberg J J, Xu X L, Irvine A C and Williams D A 2017 *Phys. Rev. B* **95** 201304
[49] Ostapenko I A, Honig G, Kindel C, Rodt S, Strittmatter A, Hoffman A and Bimberg D 2010 *Appl. Phys. Lett.* **90** 063103
[50] Torma P and Barnes W L 2015 *Rep. Prog. Phys.* **78** 013901
[51] Yang J K 2011 *Jpn. J. Appl. Phys.* **50** 060205
[52] Diniz L O, Marega E, Nunes F D and Borges B H V 2011 *J. Opt.* **13** 115001
[53] Wu Y, Li X, Duan L M, Steel D G and Gammon D 2006 *Phys. Rev. Lett.* **96** 087402